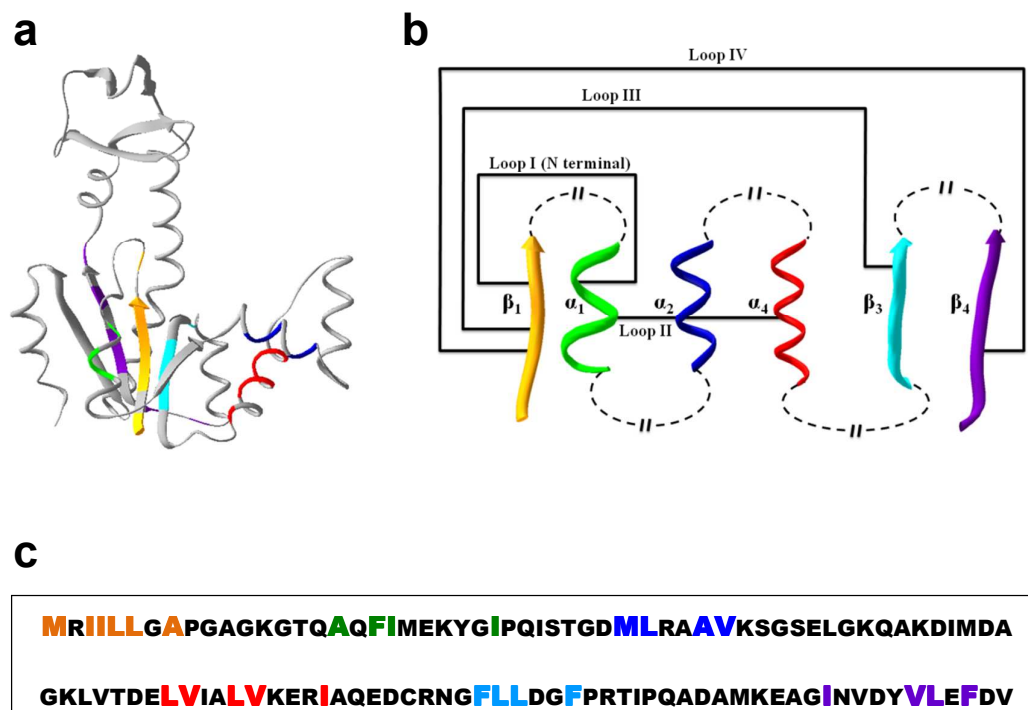


Supplementary Information to:

**Fast closure of N terminal long loops but slow formation of β strands
precedes the folding transition state of *E. coli* adenylate kinase**

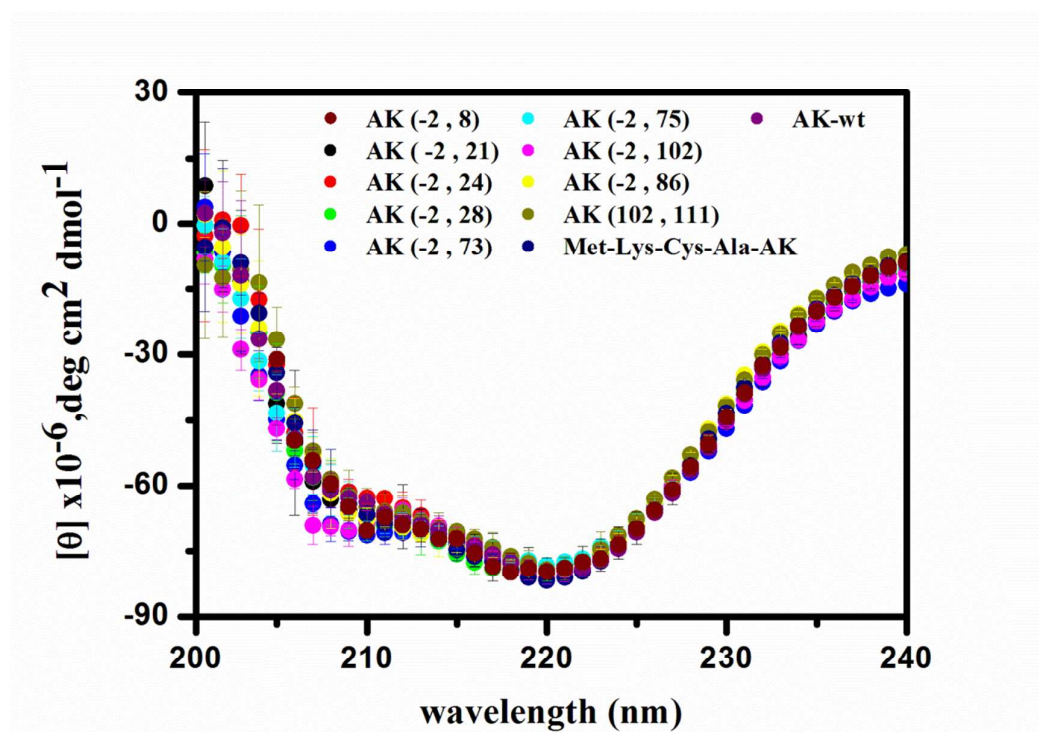
Tomer Orevi, Eldad Ben Ishay, Sivan Levin Gershanov, Mayan Ben Dalak, Dan Amir
and Elisha Haas

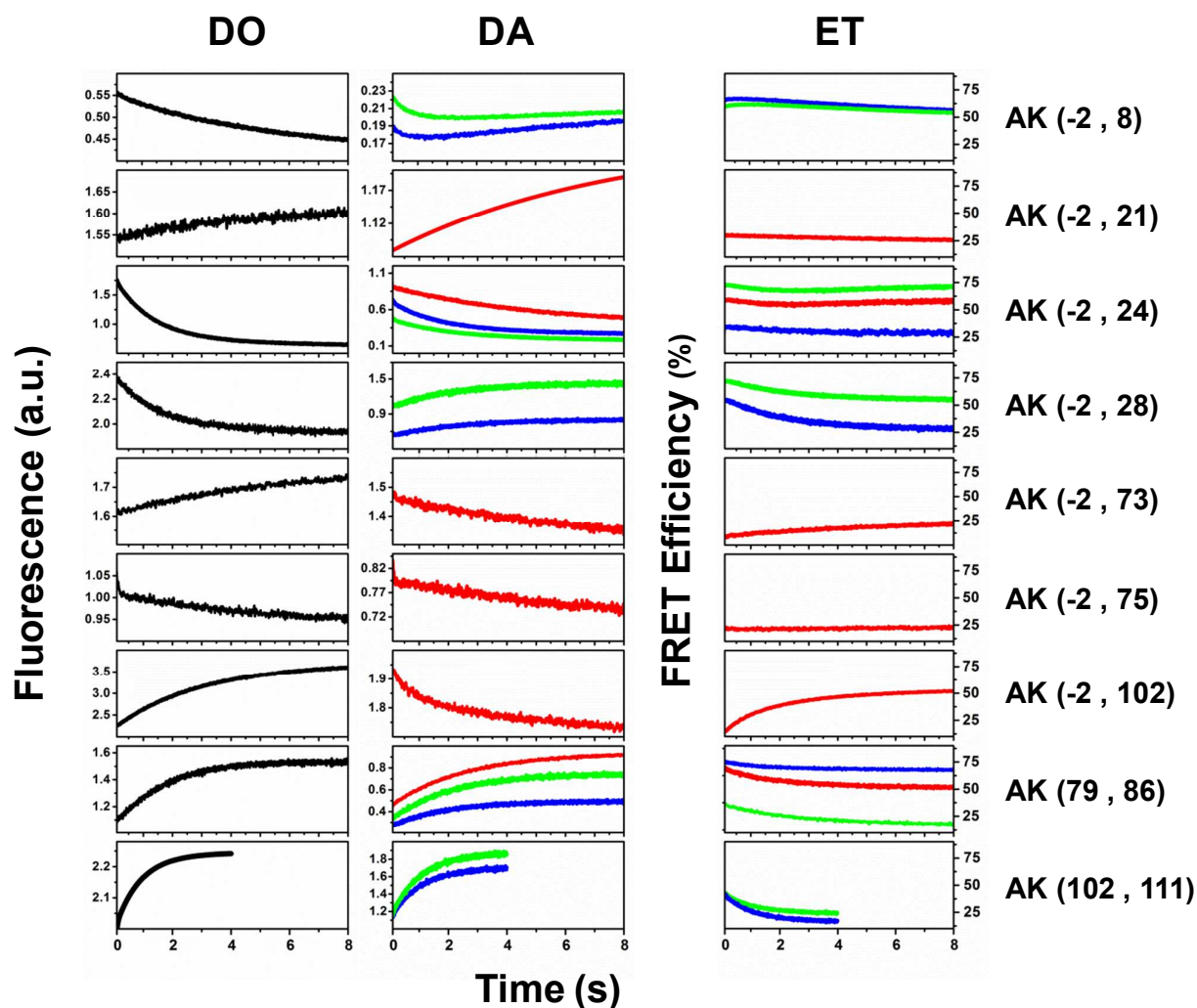
The Goodman Faculty of Life Sciences Bar Ilan University, Ramat Gan Israel 52900



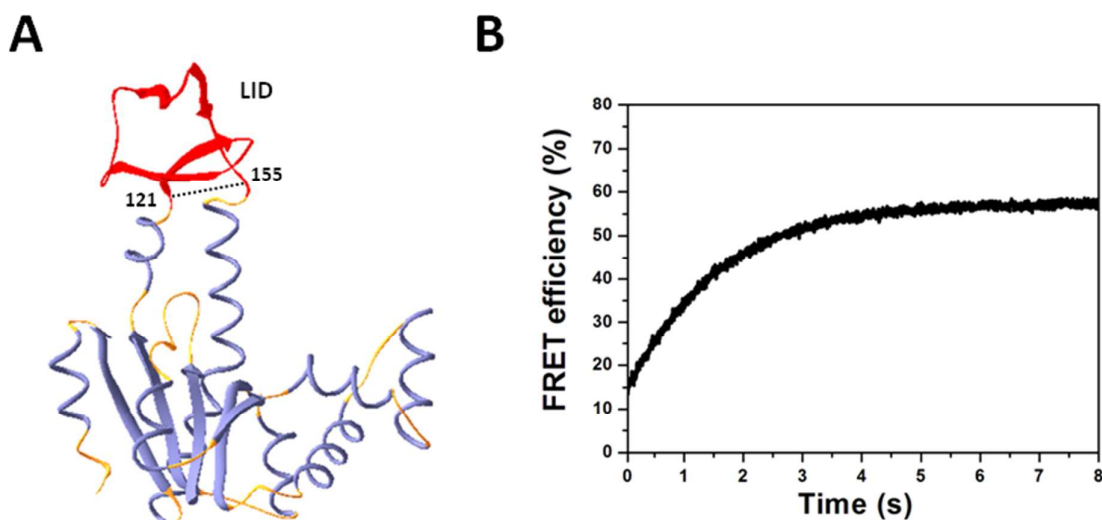
Supplementary Figure 1 schematic representation of loop structures in the CORE domain of the AK molecule. **(a)** The backbone fold of the AK molecule (PDB 4AKE). The hydrophobic clusters of residues involved in the formation of the non-local contacts that form the nodes of the closed loops are colored. **(b)** Schematic representation of the native structure loops formed by the chain segments that connect the interacting clusters. **(c)** The amino acid sequence of the N terminal section of the AK molecule highlighting the clusters of hydrophobic residues that form the loop nodes (color coded as in (a) and (b)).

Supplementary Figure 2 Far-UV CD spectra of wt-AK and its labeled mutants. The overlap of all the spectra indicates that for all the mutants the labeling modifications did not perturb the secondary structure composition of the AK molecule. Protein concentrations were 15 μ M in 20 mM Tris-HCl, pH 7.8, at 25 $^{\circ}$ C.

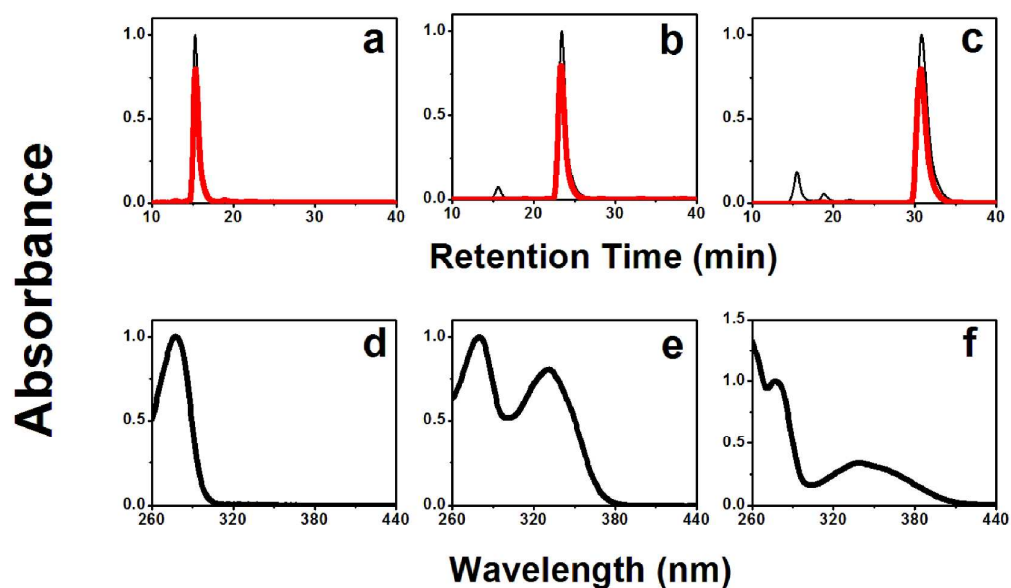




Supplementary Figure 3 Traces of the kinetics of changes of the emission intensity of the Trp residue (the donor) in each mutants during the full duration of the refolding transition and the kinetic of change of the mean transfer efficiency between the ends of the labeled segment in each mutant. Each row presents the data obtained for one mutant. The kinetics of the change of the emission intensity of the donor in the absence of the acceptor (the DO experiment) is shown in the left column and that of the donor in the presence of the acceptor (the DA experiment) is shown in the central column. When the DA experiment was repeated with more than one acceptor the traces are color coded (Sal —, coumarin —, AEDANS —). The experiments monitoring the FRET efficiency between residue -2 and 21, 24, 73 and 75 was changed by less than 10% during the full folding transition. These results show the fast closure of the loops.



Supplementary Figure 4 Refolding kinetics of a slow closed loop segment. (a) Ribbon diagram of the *E.coli* adenylate kinase highlighting the LID domain. Refolding of the LID domain was probed by labels attached to the N and C termini of this segment (position 121 and 155, respectively). The contact between residues V117 and I120 with V164 or the electrostatic interactions between clusters of charged residues in the segments 119-124 and 158-162 form a node that closes this loop. Folding kinetics was examined by the change of FRET efficiency as described throughout the text. (b) The change of FRET efficiency between the labeled sites (residues 121 and 155) near the node of the long loop of the LID domain during the refolding transition of AK. Native state FRET efficiency was recovered with a rate that characterizes the slow (rate limiting) cooperative transition of AK. Thus this is an example of a closed long loop that is not fast folding.



Supplementary Figure 5 Typical chromatographic analysis of a double-labeled AK mutant. Mono Q chromatograms of AK-D_{ONLY} (-2 , 28) (a) , AK-DA_{Cca} (-2 , 28) (b) and AK-DA_{AEDANS} (-2 , 28) (c). Absorbance was monitored at wavelength 280 nm. The black traces (a-c) illustrate analytical runs taken immediately after the labeling procedure. The red traces demonstrate the purity of the labeled samples after removal of impurities by preparative Mono Q chromatography. Absorbance spectra of the purified sample: AK-D_{ONLY} (-2 , 28), AK-DA_{Cca} (-2 , 28) and AK-DA_{AEDANS} (-2 , 28) are shown in panels d, e and f, respectively.

Supplementary table S1 relative enzymatic activity of the labeled AK mutants given in percent activity relative to that of wild type AK.

Mutant	Activity
AK-W.T.	100
AK - insert	76 ± 3
AK-(-2_{AA} 21_{Trp})	9 ± 1
AK-(-2_{AA} 24_{Trp})	59 ± 4
AK-(-2_{AA} 28_{Trp})	27 ± 5
AK-(-2_{AA} 73_{Trp})	32 ± 3
AK-(-2_{AA} 75_{Trp})	52 ± 8
AK-(-2_{AA} 102_{Trp})	73 ± 2
AK-(-2_{AA} 8_{Trp})	23 ± 2
AK-(79_{AA} 86_{Trp})	26 ± 3
AK-(102_{AA} 111_{Trp})	0

Supplementary Table S2 Rate constants obtained by different probes during the refolding transition of the mutants under study

Segment	Mutant	k_1 (s ⁻¹)	Amp ₁ (%)	k_2 (s ⁻¹)	Amp ₂ (%)
AK (-2 , 21)	DO ^a	0.2 (0.20-0.22)			
	DA _{Sal} ^b	0.1 (0.12-0.14)			
	ET _{Sal} ^c	0.1 (0.09-0.11)			
	ANS _{IAA} ^d	0.1 (0.10-0.12)			
	ANS _{Sal} ^d	0.1 (0.07-0.09)			
AK (-2 , 24)	DO ^a	0.5 (0.51-0.54)	58 (55.4-59.5)	1.2 (1.16-1.22)	42 (39.8-44.8)
	DA _{Sal} ^b	0.2 (0.15-0.17)	85 (81.5-87.8)	0.5 (0.02-0.06)	15 (11.3-18.8)
	DA _{Cca} ^b	0.4 (0.42-0.44)	71 (69.8-73.0)	12.8 (12.24-13.29)	29 (27.8-29.8)
	DA _{AEDANS} ^b	0.5 (0.52-0.54)	73 (70.3-74.7)	11.8 (11.35-12.26)	27 (26.5-28.2)
	ET _{Sal} ^c	0.2 (0.11-0.34)	31 (28.1-33.7)	0.1 (0.12-0.14)	69 (67.2-71.2)
	ET _{Cca} ^c	0.5 (0.42-0.64)	45 (41.8-46.3)	0.2 (0.17-0.23)	55 (53.0-57.4)
	ET _{AEDANS} ^c	0.2 (0.17-0.23)	58 (53.7-59.4)	0.9 (0.79-0.95)	42 (40.5-44.8)
	ANS _{IAA} ^d	0.3 (0.33-0.35)			
	ANS _{AEDANS} ^d	0.3 (0.25-0.27)			
AK (-2 , 28)	DO ^a	0.6 (0.62-0.64)			
	DA _{Cca} ^b	0.4 (0.40-0.42)			
	DA _{AEDANS} ^b	0.5 (0.44-0.45)			
	ET _{Cca} ^c	0.4 (0.43-0.45)			
	ET _{AEDANS} ^c	0.5 (0.46-0.48)			
	ANS _{IAA} ^d	0.2 (0.18-0.20)	74 (70.5-76.2)	0.8 (0.69-0.89)	26 (23.9-28.7)
AK (-2 , 73)	DO ^a	0.2 (0.16-0.18)			
	DA _{Sal} ^b	0.3 (0.22-0.29)	22 (18.5-24.4)	0.1 (0.04-0.06)	78 (76.5-80.1)

	ET_{Sal}^c	0.1 (0.11-0.13)			
	ANS_{IAA}^d	0.1 (0.09-0.11)			
	ANS_{Sal}^d	0.1 (0.07-0.09)			

Supplementary Table 1 (continued)

AK (-2 , 75)	DO^a	0.1 (0.10-0.12)			
	DA_{Sal}^b	0.1 (0.10-0.12)			
	ET_{Sal}^c	0.1 (0.09-0.11)			
	ANS_{IAA}^d	0.2 (0.14-0.16)			
	ANS_{Sal}^d	0.1 (0.08-0.10)			
AK (-2 , 102)	DO^a	0.3 (0.33-0.35)			
	DA_{Sal}^b	0.2 (0.16-0.18)	56 (54.7-58.2)	1.6 (1.52-1.65)	44 (43.0-44.4)
	ET_{Sal}^c	0.3 (0.31-0.33)	62 (59.4-63.8)	1.2 (1.14-1.18)	38 (37.8-39.0)
	ANS_{IAA}^d	0.3 (0.26-0.28)	86 (84.6-87.1)	0.1 (0.04-0.06)	14 (10.1-16.8)
	ANS_{Sal}^d	0.2 (0.16-0.18)			
AK (-2 , 8)	DO^a	0.3 (0.33-0.35)			
	DA_{Cca}^b	0.2 (0.15-0.17)	82 (80.4-85.7)	4.0 (3.73-4.32)	18 (15.5-19.4)
	DA_{AEDANS}^b	0.2 (0.19-0.21)	35 (33.0-37.5)	2.5 (2.39-2.59)	65 (62.9-66.1)
	ET_{Cca}^c	0.1 (0.12-0.14)	93 (91.0-95.6)	5.9 (3.06-8.76)	7 (2.1-15.2)
	ET_{AEDANS}^c	0.1 (0.11-0.13)	84 (80.1-86.2)	3.5 (3.21-3.83)	16 (12.9-19.2)
	ANS_{IAA}^d	0.1 (0.13-0.15)	82 (80.4-85.7)	4.0 (3.73-4.32)	18 (15.5-19.4)
	ANS_{Cca}^d	0.1 (0.11-0.13)			
AK (79 , 86)	DO^a	0.6 (0.58-0.60)			
	DA_{Sal}^b	0.4 (0.39-0.41)			
	DA_{Cca}^b	0.5 (0.53-0.55)			
	DA_{AEDANS}^b	0.5 (0.48-0.50)			
	ET_{Sal}^c	0.3 (0.33-0.35)			
	ET_{Cca}^c	0.6 (0.59-0.61)			

ET_{AEDANS}^c	0.5 (0.50-0.52)			
ANS_{IAA}^d	0.6 (0.55-0.58)			

Supplementary Table 1 (continued)

AK (102 , 111)	DO^a	1.3 (1.25-1.27)			
	DA_{Cca}^b	0.9 (0.91-0.94)	87 (84.2-88.1)	5.1 (4.35-5.74)	13 (11.9-15.2)
	DA_{AEDANS}^b	1.0 (0.97-0.99)	83 (81.1-84.0)	13.0 (10.84-15.11)	17 (13.9-20.2)
	ET_{Cca}^c	0.8 (0.77-0.84)	75 (71.1-77.3)	2.9 (10.84-15.11)	25 (22.2-28.6)
	ET_{AEDANS}^c	1.0 (0.96-0.99)	83 (80.1-85.5)	8.6 (7.22-10.01)	17 (14.8-18.9)
	ANS_{IAA}^d	No binding			

Each block summarizes the kinetic data for a specific segment. All traces could be well fitted to a single or biphasic exponential function.

^a Exponential fit to the observed change in the total fluorescence of tryptophan in the absence of an acceptor, during refolding.

^b Exponential fit to the observed change in the total fluorescence of tryptophan in the presence of the indicated acceptor, during refolding.

^c Exponential fit to the calculated change of transfer efficiency of the indicated FRET pair.

^d Exponential fit to the observed change in the total fluorescence of ANS, during refolding.

The change of tryptophan fluorescence in the DO mutant (**a**) is sensitive to changes in the local environment near the indole ring. The change of tryptophan fluorescence in the DA mutant (**b**) reports on both local changes in the environment and the effect of FRET. The change of ANS fluorescence probes the binding of ANS to a transient intermediate state and the subsequent release of ANS as folding progresses.

Supplementary Table S3 Mean fluorescence lifetime of the tryptophan residue in the single (DO) and double (DA) labeled mutants of AK under folding and denaturing conditions at equilibrium

Mutant	Gnd-HCl 0.3 M				Gnd-HCl 2 M			
	IAA ^a	Sal ^b	Cca ^c	AEDANS ^d	IAA ^a	Sal ^b	Cca ^c	AEDANS ^d
AK (-2 , 21)	3.3	2.5	N.D.	N.D.	1.7	1.6	N.D.	N.D.
AK (-2 , 24)	0.7	0.45	0.2	0.3	2.7	2.5	1.8	1.8
AK (-2 , 28)	2.2	N.D.	1	1.6	2.9	N.D.	1.8	2.2
AK (-2 , 73)	4.2	3	N.D.	N.D.	2.1	2.4	N.D.	N.D.
AK (-2 , 75)	2.1	1.6	0.6	N.D.	2	2	1.9	N.D.
AK (-2 , 102)	6.1	2.8	N.D.	N.D.	3	2.6	N.D.	N.D.
AK (-2 , 8)	2.5	N.D.	1.4	1.4	2.1	N.D.	0.6	0.9
AK (79 , 86)	2.5	2.1	0.8	1.2	2.3	1.3	0.5	0.6
AK (102 , 111)	4.1	N.D.	3.1	3.4	2.8	N.D.	1.2	1.4

^a The mean lifetime of the tryptophan residue in the absence of an acceptor reflects wide range of variation, which depends mainly on the local environment of the indole moiety . Note the small range of variation when the lifetime of the tryptophan residues was measured in high Gnd-HCl concentration. The tryptophan inserted at residue 24 is strongly quenched in the native state (probably by interaction with Methionine 1 and Lysine 23), and the lifetime is tripled in the high Gnd-HCl solution where the contact quenching is probably reduced. Note the 6.1 ns lifetime of the tryptophan inserted at position 102, which is reduced by 50% in the high Gnd-HCl solution, where the unique (hydrophobic) local environment of residue 102 is lost.

^{b-d} Three different acceptor probes used in the labeling plan resulted in double labeled mutants with slightly different characteristics.